JVSTB Journal of Vacuum Science & Technology B

Atomic precision lithography on Si

J. N. Randall, J. W. Lyding, S. Schmucker, J. R. Von Ehr, J. Ballard, R. Saini, H. Xu, and Y. Ding

Citation: Journal of Vacuum Science & Technology B **27**, 2764 (2009); doi: 10.1116/1.3237096
View online: http://dx.doi.org/10.1116/1.3237096
View Table of Contents: http://scitation.aip.org/content/avs/journal/jvstb/27/6?ver=pdfcov
Published by the AVS: Science & Technology of Materials, Interfaces, and Processing

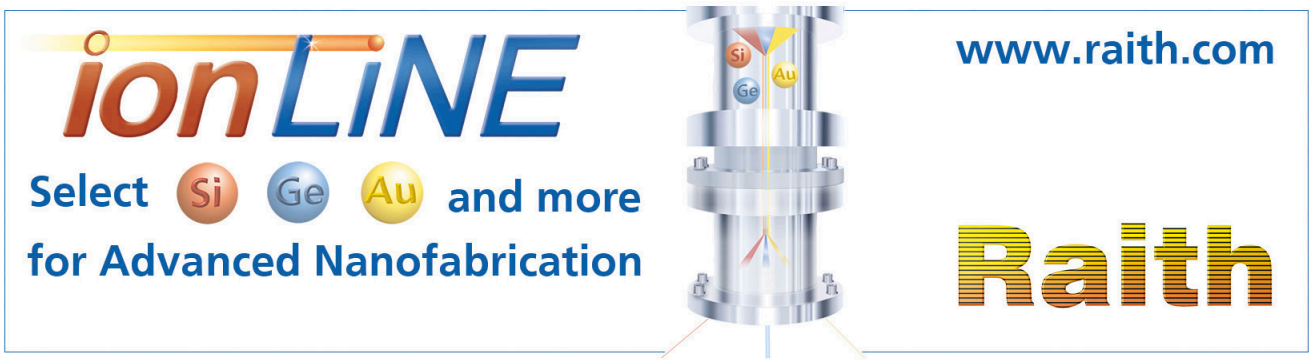

Atomic precision lithography on Si

J. N. Randall[a)]
Zyvex Labs, 1321 North Plano Rd., Richardson, Texas 75081

J. W. Lyding and S. Schmucker
University of Illinois at Urbana-Champaign, 405 North Mathews Ave., Urbana, IL 61801

J. R. Von Ehr, J. Ballard, and R. Saini
Zyvex Labs, 1321 North Plano Rd., Richardson, Texas 75081

H. Xu and Y. Ding
Zyvex Asia, 10 Anson Rd., #09–24 International Plaza, Singapore, 079903

(Received 1 July 2009; accepted 10 August 2009; published 2 December 2009)

Lithographic precision is as or more important than resolution. For decades, the semiconductor industry has been able to work with ±5% precision. However, for other applications such as micronanoelectromechanical systems, optical elements, and biointerface applications, higher precision is desirable. Lyding *et al.* [Appl. Phys. Lett. **64**, 11 (1999)] have demonstrated that a scanning tunneling microscope can be used to remove hydrogen (H) atoms from a silicon (100) 2 × 1 H-passivated surface through an electron stimulated desorption process. This can be considered e-beam lithography with a thin, self-developing resist. Patterned hydrogen layers do not make a robust etch mask, but the depassivated areas are highly reactive since they are unsatisfied covalent bonds and have been used for selective deposition of metals, oxides, semiconductors, and dopants. The depassivation lithography has shown the ability to remove single H atoms, suggesting the possibility of precise atomic patterning. This patterning process is being developed as part of a project to develop atomically precise patterned atomic layer epitaxy of silicon. However, significant challenges in sample preparation, tip technology, subnanometer pattern placement, and patterning throughput must be overcome before an automated atomic precision lithographic technology evolves. © *2009 American Vacuum Society.* [DOI: 10.1116/1.3237096]

I. INTRODUCTION

Scanning probe microscopes have high spatial resolution and have been used for atomic and molecular manipulation almost since their inception.[1] However, the physical manipulation of atoms and molecules has a number of practical problems that have largely limited this sort of use to laboratory experiments. The use of electrons transferring between tip and sample in a scanning tunneling microscope can be used for patterning similar to focused electron beams.[2] While exposure of conventional e-beam resists[3] and electron induced surface reactions[4] are possible patterning approaches, they typically require electron energies in excess of 5 eV which typically puts a scanning tunneling microscopy (STM) in a field emission mode rather than a tunneling mode limiting their resolution to approximately 5 nm presumably because the electrons emitted from the tip are diverging from the tip and have an effective spot size limitation of 5 nm or larger.

This article will investigate the use of a STM to do lithography via electron induced desorption from a Si (100) 2 × 1 H passivated surface. When prepared properly in ultrahigh vacuum (UHV) the silicon (100) surface reconstructs into dimer rows where surface Si atoms share one of their two unsatisfied covalent bonds with a neighboring silicon atom.[5] In this way each surface Si atom has one dangling bond that can be passivated with a hydrogen (H) atom. It is these H atoms that can be removed via electron stimulated desorption using electrons from the STM tip. A recent review article by Walsh and Hersam[2] provides an excellent overview of the state of the art of H-depassivation lithography. There are two distinct modes of this type of lithography. The higher bias mode (6–10 V) is in the field emission regime where the yield is approximately 2×10^6 electrons/(desorbed H-atom) and is independent of current indicating that a single electron can break the Si–H bond, but that the cross section for such an energy transfer is very small. As mentioned above, the resolution in this mode is approximately 5 nm and typically produces some line edge roughness. Lyding *et al.* first demonstrated that in tunneling mode (biases at ~4 V and below) it was possible to remove H atoms from a Si (100) 2 × 1 H-passivated surface with atomic resolution.[6] In this mode the individual electrons tunneling from the tip to sample lack sufficient energy to beak the Si–H bond but can vibrationally heat the H atom until it has gained the required energy to desorb from the Si surface. In a competing process, bulk phonons in the Si lattice can quench the excited state back to the ground state. This competition results in a current dependence to the yield. There is some disagreement in the literature with respect to the number of electrons required to transfer enough energy through inelastic scattering for H desorption,[7,8] but in any case the yield at 3 V with a 2 nA current is 100 times worse than the field emission mode.

a)Electronic mail: jrandall@zyvexlabs.com

TABLE I. Comparison of high resolution exposure processes.

Technique	Bias	Current (nA)	Resist	Sensitivity	μm^2 exposure time
E-Beam	10 kV	0.2	10 nm HSQ	~1 mC/cm^2	0.05 s
FE STM	8 V	1.0	Monolayer H	53 C/cm^2	4.5 min
Tunneling STM	3 V	2.0	Monolayer H	5300 C/cm^2	7.4 h

These yields are very low and result in extremely high doses even when compared to a relatively slow high resolution e-beam lithography exposure technique. Table I compares the required dose of conventional e-beam lithography,[9] the field emission mode of H-depassivation lithography,[8] and the atomic resolution mode of H-depassivation lithography.[8] This should make abundantly clear that this lithography process is not going to be suitable for integrated circuits. However, there is the promise of essentially perfect patterning and the exposed dangling bonds on the Si surface have been used for selective deposition of a wide variety of materials.[2] This article will explore the possibility of developing an automated H-depassivation lithography process with atomic precision.

II. LITHOGRAPHY EXPERIMENTS

A highly boron doped (*n*-type) Si (100) wafer (resistivity of ~0.01–0.02 Ω cm) went through a RCA cleaning procedure as the first step. The wafer was diced into die size of 5×8 mm^2 and solvent cleaned. After introduction to UHV, the sample was degassed at 600 °C for 8–10 h. Samples were flashed to 1200C for 30 s, with subsequent 1200C flashes for 10 and 5 s. For H passivation the sample was maintained at 377 °C in the presence of a 1300 °C tungsten filament and hydrogen background (2×10^{-6} Torr) for 10 min. First, the samples were imaged in a home built STM described elsewhere.[10] Using STM imaging at a sample bias of 2 V and a current of 50 pA, an atomically flat area without dangling bonds or other defects was located. Because of the nonlinear current dependence of the depassivation yield at this low bias, there is an extremely low probability of depassivation while imaging. Next, a line dose of 2 mC/cm was delivered with a sample bias of +4 V and a current of 2 nA along dimer rows. The tip was intended to pass along the center of the dimer row at a constant rate based on the last recorded image. No attempt to use the tunneling current for control of the litho process was made during the exposure other than the usual tip height adjustments to attempt to maintain a constant current.

Figure 1 shows the two best results to date. In each case the results are close to perfect patterning, but there are a few defects. The STM images show the counterintuitive feature that the removed H atom appears as a raised topographical feature because of the increased tunneling efficiency into the dangling bond[11] created by the removed H. Figure 1(a) is displayed in the derivative mode and Fig. 1(b) is in the topographical mode. In both images we have added circles to better indicate where H atoms have been removed. In Fig. 1(a) one dimer had only one of the H atoms removed and the two dimer rows are of different length. In Fig. 1(b) all 44 H atoms along the two dimer rows were removed forming a 4.26×1.55 nm^2 rectangle. However, one additional H atom on a neighboring dimer row was inadvertently removed.

Laboratory demonstrations such as these are interesting and useful for a few experiments, but are far less useful than a robust and automated lithography process that can be used to produce perfect or near perfect patterns. Significant challenges in sample preparation, tip technology, subnanometer pattern placement, and automated process control must be met for this to be possible. Sample preparation will not be discussed in this article as current methods are adequate for developing a lithography process.

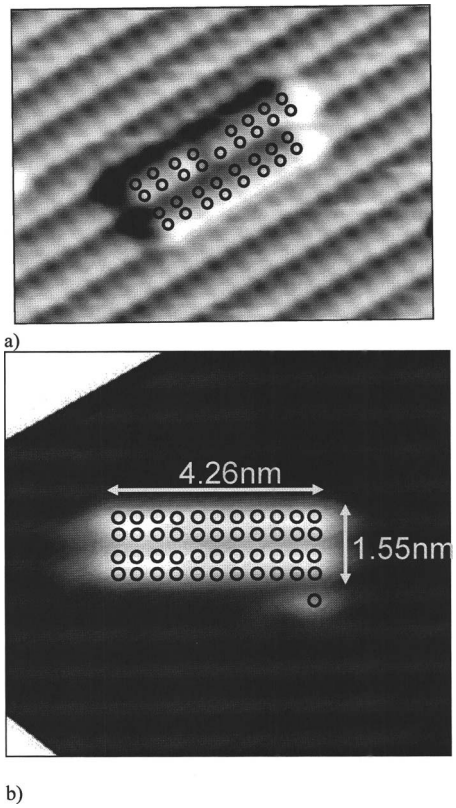

FIG. 1. (a) STM image (differentiated mode) of a Si (100) 2 × 1 H passivated surface where H was removed by STM lithography using an electrochemically etched and sputter sharpened W tip. (b) A STM image (topographical mode) of a Si (100) 2 × 1 H passivated surface where H was removed by STM lithography using an electrochemically etched and sputter sharpened HfB_2 tip. In both cases the STM delivered a 2 mC/cm dose along dimer rows at a sample bias of 4 V and current of 2 nA. In both figures the removal of H atoms are highlighted by circles.

III. TIP TECHNOLOGY

The most uncontrolled factor in STM imaging and patterning is the tip. While atomic resolution imaging simply requires a single atom be closer to the surface than any other part of the tip so that the tunneling current passes predominantly through that single atom, most STM tips need to be processed by one of several methods to "prepare" it for imaging and often require additional processing periodically to maintain atomic resolution imaging.[12] The processes for tip degradation during imaging are not well understood, but presumably, any physical contact with the surface will perturb the tip by rearranging the critical tip atoms or pick up atoms from the surface. Physical contact with the surface is not required for other processes to perturb the tip. The high fields and large current densities associated with STM operation can attract materials and cause surface migration of atoms on the tip.

For reproducible atomic precision lithography the physical requirements are far more restrictive and the conditions are more extreme. The significantly higher currents will result in closer tip spacing and consequently higher fields. While there is disagreement in the literature[13] on the importance of the field in the depassivation process, a physically sharp tip on the nanoscale will have advantages in maintaining the resolution of the process and a sharper tip with its inherent field intensification will allow larger tip to sample distances and better confinement of the electric field, both of which will reduce possible tip degradation processes. On the other hand a sharper tip will likely be less robust due to enhanced possibility of surface migration and degraded structural strength.

A single atom tip with a reproducible atomic structure around that single atom is an attractive target for an invariant STM tip, and a number of technologies are known to produce single atom tips on W wires.[14–16] There is also the opportunity to better understand the lithography process by modeling the tips.[17] However, a single atom tip may not be robust enough for an automated lithography process. Furthermore, the priority is on atomic resolution patterning, not imaging. Note in Fig. 1(a) that individual dimers are clearly imaged, but that in Fig. 1(b) that only dimer rows are resolved but not dimers. This tip was produced by field directed sputter sharpening[18] approach that is a self-limiting process that produces very sharp apex structures (~2 nm radius of curvature).

Some level of imaging resolution will be required but probably not atomic. Dimer row resolution may be adequate. On the other hand, better resolution, higher contrast imaging will improve pattern placement. Further studies will be required to define an optimized tip structure.

IV. PATTERN PLACEMENT

High resolution lithography processes generally require accurate pattern placement. Image drift is an accepted feature in STM imaging. While efforts to minimize drift are important, some drift correction mechanism is likely to be required. Drift correction usually involves referring to a fiducial mark (or marks) periodically. Adding fiducial marks that survive high temperature sample preparation can be achieved, but require large marks that would be problematic to image with a STM.[19] We developed a drift correction method that calculates a translational mismatch parameter between sequential scans followed by the application of an intelligent correction factor.

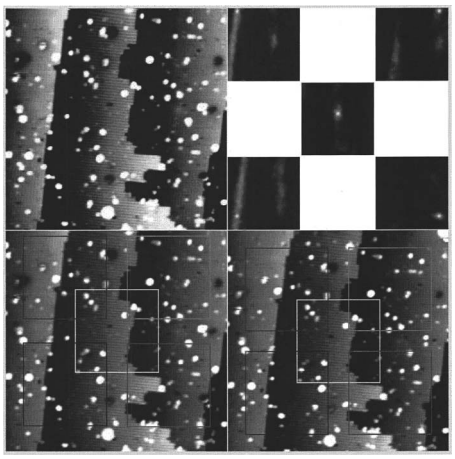

FIG. 2. Cross correlation between current and previous scans showing the five regions of interest.

In order to accommodate variations in the raw data on which the drift correction algorithm works, we first preprocess each image. By using line by line tilt correction or least squares plane fit subtraction followed by a renormalization of the image histogram, we optimize the robustness of the routines.[20] Upon completion of the second and all subsequent scans after drift correction is enabled, each scan (Scan_N) is compared to the previous scan (Scan_{N-1}).

The comparison mechanism between Scan_N and Scan_{N-1} consists of cross correlations between five preset regions of interest (ROIs) on Scan_{N-1} and nearby regions on Scan_N. Each ROI is 3/8 the size of the whole scan and is chosen from the center of four quadrants and the origin of Scan_{N-1} (bottom right in Fig. 2) to minimize the impact of piezocreep and tip condition change. Individually, these ROIs "slide" over the Scan_N (bottom left in Fig. 2) to maximize the cross correlation between scans, yielding up to five pixel drifts (Drift_i) between scans. The match score for each ROI ($\mathrm{MatchScore}_i$) (as determined by the brightest spot of the cross correlation shown in Fig. 2 top right corner) will be compared with a user-specified threshold to confirm a pair of matched ROIs. Finally, the weighted drift of two scans is calculated by

$$\mathrm{Drift}_{\mathrm{weighted}} = \frac{\Sigma_{i=1}^{n}\mathrm{Drift}_i(\mathrm{MatchScore}_i - \mathrm{Threshold})}{\Sigma_{i=1}^{n}(\mathrm{MatchScore}_i - \mathrm{Threshold})}, \quad (1)$$

where n denotes the number of matched ROIs predefined to confirm a match between two scans, $n=5$ in Fig. 2.

The ROI matching score can be greatly affected by STM image quality. Sometimes we found that when tip or sample condition was subpar, the matching scores of the five ROIs all fell below the cutoff threshold but with pixel drift calcu-

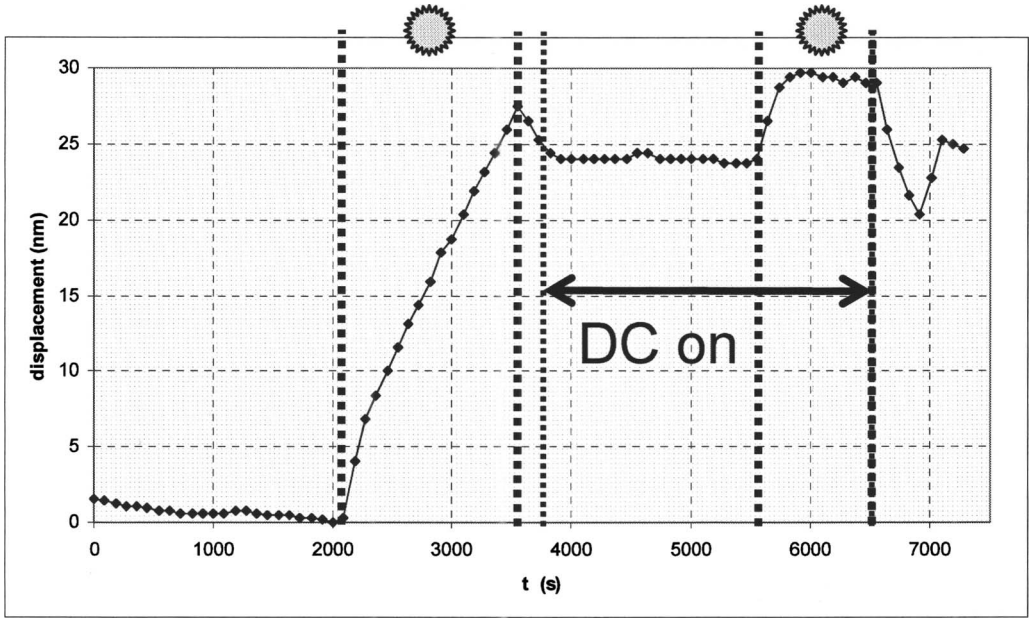

FIG. 3. Plot of displacement (nanometer) as a function of time (seconds) of a silicon surface imaged by a STM. Single STM scans were taken repeatedly lasting approximately 90 s. From ~2000 to 3600 s a halogen lamp was turned on creating a thermally induced drift. At 3800 s the drift correction was turned on. At 5600 s the lamp was turned on again. At 6500 s both the lamp and drift correction were turned off.

lations reflecting the right value. In this case, the standard deviation of the top matches is used. If the minimum standard deviation is smaller than the predefined pixel drift threshold (typically 3 pixels), then the current and previous scans can also be considered matched and weighted drift between two scans will be calculated afterward.

The drift correction routine attempts to keep the scan centered on the image seen when drift correction was turned on. To do this, it maintains a cumulative drift offset from the starting scan, adding the current frame's drift offset to that cumulative offset at each scan. It will then correct for a drift that moves away from the starting point, but not change drift settings that move back toward the starting point. In this way, drift correction acts slowly, making it easy to follow a feature from frame to frame in a video.

The digital signal processor (DSP) applies the accumulated drift correction to its fine X/Y position each time through the DSP update loop (100 000 times/s). A floating point correction factor is updated with the current delta, rounded to integer, and added to the nominal integer X/Y position. Typically, one least significant bit for the X and Y positions is scaled to move the tip 1/40 000 of the scan field, meaning that in a typical 100 nm field, one least significant bit maps to 1/400 nm, or 0.025 Å, so granularity of the correction is quite fine. Once set, the drift correction value is continually accumulated by the DSP without host computer intervention, and independently of host computer timings.

Figure 3 shows the drift as measured manually by measuring displacement of a single point of reference that was visible in all scans and measuring with respect to the location of the reference point in the first scan. In our STM system, scans are repeated every 90 s. In the first 2000 s the drift is very slow. The total drift is approximately 2 nm in that period of time. At a time slightly over 2000 s a halogen lamp outside the chamber is turned on which illuminates the STM inside the chamber creating a significant thermally induced drift. At approximately 3500 s the lamp is turned off and the drift reverses direction.

At approximately 3800 s, the automated drift correction routine is engaged. After a couple of scans the drift is effectively cancelled with very little drift measured from the point of view of image drift. At approximately 5600 s, the lamp is turned on again which begins a large thermal drift that the drift correction routine does not catch up with for a couple of scans, and then keeps the image fairly stationary until it is disengaged at 6500 s. At that same time the lamp is turned off and a relatively large drift then resumes. This demonstration in the face of a large perturbation suggests that we can effectively determine and correct for drift in the STM system without reference to fiducial marks. We note that fiducial marks are still required for alignment and other purposes. We expect that more sophisticated control loops for drift correction will track changes faster and more accurately.

Eliminating the drift is an important component of pattern placement, but scanning with piezos has its own set of nonlinearity, creep, and hysteresis problems. While there are a variety of techniques that could be used to assure accurate pattern placement, spatial phase locking using a global fiducial grid as suggested by Smith *et al.*[21] is particularly attractive because the silicon lattice provides us with just such a global fiducial grid. We expect to explore this as an approach to maintaining accurate pattern placement. Defects and the 2 $\times$1 reconstruction of the Si surface would have to be dealt with.

V. DIGITAL LITHOGRAPHY

Removing H atoms from a Si surface, where there is a single H atom passivating each surface Si atom, can be considered a digital process: the 2×1 reconstruction into dimer rows places the H atoms on a regular, addressable grid, and the H atom is either there (unwritten) or not (written). We suggest that there are parallels with patterned media for memory storage,[22] or the suggestion of Maluf and Pease[23] to create a quantized lithography media. More broadly, we maintain that all of the advantages that come with a digital technology (tolerance and error correction) can be exploited here.

The physics of H depassivation from Si surfaces provides excellent margins for a digitized approach. The presence or absence of an individual H atom in a specific location (pixel) can be detected with a very high degree of certainty. There are also very large margins between the read (imaging) and write process as mentioned earlier. As an added bonus, the write process (H desorption) is accompanied with a clear signal that is a jump in tunneling current due to increased tunneling efficiency into the newly created dangling bond. The technology for controlling the position of a tip to within 0.1 nm is available which allows individual H atoms on the Si surface (nominal spacing of 0.387 nm) to be addressed reliably. The lifetime of the dangling bond in UHV is long enough to perform interesting chemistry such as atomic layer epitaxy, but short enough that it would need to be terminated for most other applications.

VI. SCALING UP

While the physics of the writing process produce very low throughput, there are approaches to dramatically improving patterning throughput. The depassivation yields and rates stated above could be improved upon with improved tips and writing strategies. We also plan to explore a parallel tip approach with independent closed loop microelectromechanical systems (MEMSs) based *XYZ* nanopositioners. One possibility is a complementary metal oxide semiconductor compatible MEMS process has the advantage of integrating the electronics for closed loop control, tunnel current preamplification, and possibly other functions.

VII. CONCLUSIONS

STM based H depassivation from Si surfaces has the potential for atomic precision lithography. Near perfect depassivation patterns have been demonstrated in the laboratory. Several challenges including sample preparation, tip technology, subnanometer pattern placement, and automated process control must be met for this to be possible in an automated and robust process. A key advantage that can be exploited is the digital nature of this patterning process.

ACKNOWLEDGMENTS

This material is based on work supported by the Defense Advanced Research Project Agency (DARPA) and Space and Naval Warfare Center, San Diego (SPAWARSYSCEN-SD) under Contract No. N66001-08-C-2040. It is also supported by a grant from the Emerging Technology Fund of the State of Texas to the Atomically Precise Manufacturing Consortium.

[1]D. M. Eigler and E. K. Schweizer, Nature (London) **344**, 524 (1990).
[2]Michael A. Walsh and Mark C. Hersam, Annu. Rev. Phys. Chem. **60**, 193 (2009).
[3]J. Hartwich, L. Dreeskornfeld, V. Heisig, S. Rahn, O. Wehmeyer, U. Kleineberg, and U. Heinzmann, Appl. Phys. A: Mater. Sci. Process. **66**, S685 (1998).
[4]Richard Silver, Kai Li, Summanth Chikkamaranahalli, Pradeep Namboodiri, and Joe Fu, EIPBN 28 May, 2009, Marco Island Florida (unpublished).
[5]D. R. Bowler, Phys. Rev. B **67**, 115341 (2003).
[6]J. W. Lyding, T.-C. Shen, J. S. Hubacek, J. R. Tucker, and G. C. Abeln, Appl. Phys. Lett. **64**, 2010 (1994).
[7]Laetitia Soukiassian, Andrew J. Mayne, Marilena Carbone, and Gérald Dujardin, Phys. Rev. B **68**, 035303 (2003).
[8]T.-C. Shen, C. Wang, G. C. Abeln, J. R. Tucker, J. W. Lyding, Ph. Avouris, and R. E. Walkup, Science **268**, 1590 (1995).
[9]Joel K. W. Yang, Bryan Cord, Joseph Klingfus, Sung-Wook Nam, Ki-Bum Kim, Michael J. Rooks, and Karl K. Berggren, EIPBN 28 May, 2009, Marco Island Florida (unpublished); Joel Yang (private communication).
[10]Mathew Sztelle, Ph.D. thesis, University of Illinois U-C, 2008.
[11]M. C. Hersam, N. P. Guisinger, and J. W. Lyding, Nanotechnology **11**, 70 (2000).
[12]Anne-Sophie Lucier, M.S. thesis, McGill University Montréal, 2004.
[13]X. Tong and R. A. Wolkow, Surf. Sci. **600**, L199 (2006).
[14]Hong-Shi Kuo, Ing-Shouh Hwang, Tsu-Yi Fu, Yu-Chun Lin, Che-Cheng Chang, and Tien T. Tsong, e-J. Surf. Sci. Nanotechnol. **4**, 233 (2006).
[15]Moh'd Rezeq, Jason Pitters, and Robert Wolkow, J. Chem. Phys. **124**, 204716 (2006).
[16]H.-W. Fink, IBM J. Res. Dev. **30**, 460 (1986).
[17]HeeSung Choi, Min Huang, J. B. Ballard, K. T. He, S. W. Schmucker, J. W. Lyding, J. N. Randall, and Kyeongjae Cho, MRS Spring Meeting 2009 (unpublished).
[18]Joseph W. Lyding and Scott Schmucker, U.S. Patent Application No. 20080105539 (pending).
[19]Martin Fuechsle, Frank J. Rueβ, Thilo C. G. Reusch, Mladen Mitic, and Michelle Y. Simmons, J. Vac. Sci. Technol. B **25**, 2562 (2007).
[20]Gary Bradski and Adrian Kaebler, *Learning OpenCV. Computer Vision With The OpenCV Library*, 1st ed. (O'Reilly Media Inc., Sebastopol, CA, 2008).
[21]Henry I. Smith, Scott D. Hector, M. L. Schattenburg, and Erik H. Anderson, J. Vac. Sci. Technol. B **9**, 2992 (1991).
[22]B. D. Terris, T. Thomson, and G. Hu, Microsyst. Technol. **13**, 189 (2007).
[23]Nadim I. Maluf and R. Fabian Pease, J. Vac. Sci. Technol. B **9**, 2986 (1991).